

# THE SECOND US NAVAL OBSERVATORY CCD ASTROGRAPH CATALOG (UCAC2)

N. Zacharias, S. E. Urban, M. I. Zacharias<sup>1</sup>, G. L. Wycoff, D. M. Hall, D. G. Monet<sup>2</sup>  
and T. J. Rafferty

*U.S. Naval Observatory, 3450 Mass. Ave. NW, Washington, DC 20392*

`nz@usno.navy.mil`

## ABSTRACT

The second USNO CCD Astrograph Catalog, UCAC2 was released in July 2003. Positions and proper motions for 48,330,571 sources (mostly stars) are available on 3 CDs, supplemented with 2MASS photometry for 99.5% of the sources. The catalog covers the sky area from  $-90^\circ$  to  $+40^\circ$  degrees declination, going up to  $+52^\circ$  in some areas; this completely supersedes the UCAC1 released in 2001. Current epoch positions are obtained from observations with the USNO 8-inch Twin Astrograph equipped with a 4k CCD camera. The precision of the positions are 15 to 70 mas, depending on magnitude, with estimated systematic errors of 10 mas or below. Proper motions are derived by utilizing over 140 ground-and space-based catalogs, including Hipparcos/Tycho, the AC2000.2, as well as yet unpublished re-measures of the AGK2 plates and scans from the NPM and SPM plates. Proper motion errors are about 1 to 3 mas/yr for stars to 12th magnitude, and about 4 to 7 mas/yr for fainter stars to 16th magnitude. The observational data, astrometric reductions, results, and important information for the users of this catalog are presented.

*Subject headings:* astrometry – catalogs – stars: kinematics – method: data analysis

## 1. INTRODUCTION

The U.S. Naval Observatory (USNO) operates the 8-inch Twin Astrograph (Douglass & Harrington (1990); Zacharias & Zacharias (1999)) currently from its Flagstaff station (NOFS). The program currently underway with this instrument is the USNO CCD Astrograph Catalog project; it is an ongoing program which started at the Cerro Tololo Interamerican Observatory (CTIO) in 1998. Completion of the all-sky, astrometric observations are expected in May 2004. This second data release, the UCAC2, is a substantial increase in data volume and includes improvements of reduction techniques over the first release, UCAC1, as described in Paper I (Zacharias

et al. 2000). The UCAC2 encompasses the entire area of UCAC1 and completely supersedes it. The sky coverage has about doubled and new measurements were obtained from early epoch plates that are used in UCAC2 to significantly improve the proper motions with respect to the UCAC1 release.

The goal of this project is the densification of the reference frame at optical wavelengths; see also Zacharias (2002). Toward this goal, UCAC provides about a factor of 30 more stars per square degree than the Tycho-2 catalog. The precision of the UCAC observed positions comes close to the precision of Hipparcos positions at current epochs, and surpasses the precision of Tycho-2 positions at about 10th magnitude and fainter. The UCAC2, a compiled catalog, includes Hipparcos and Tycho observational data as well as virtually all ground-based catalogs used for the Tycho-2 proper motions. Thus, within the sky area covered, UCAC2

<sup>1</sup>also with Universities Space Research Association, USRA, Washington, DC

<sup>2</sup>at the Naval Observatory Flagstaff Station (NOFS), Arizona

supersedes the Tycho-2 astrometry for stars 10th magnitude and fainter, providing the most precise positions and proper motions available today for catalogs of comparable area coverage.

Users should note some UCAC limitations. Stars brighter than about  $R = 10$ , and in particular those brighter than  $R = 9$ , can suffer from overexposure effects and generally are based on 2 images of short exposures only. Their errors are higher and this is reflected in the catalog; they should be used with caution when the strictest astrometry is required. The UCAC observations provide only crude magnitudes in a single, non-standard bandpass (between V and R). To make the catalog more useful to the astronomy community, the Two Micron All Sky Survey (Cutri et al. 2003) J, H, and  $K_S$  infrared magnitudes are included for the matched sources (99.5% of the total UCAC sources). UCAC2 does not provide any trigonometric parallaxes. Systematic errors in the UCAC2 positions are 5 to 10 mas; although very small, these are larger than in the Hipparcos Catalogue.

Along with UCAC2 superseding UCAC1, users should note that the UCAC1 was an observational catalog with attached, preliminary proper motions. UCAC2 is a compiled catalog of positions and proper motions referred to a standard epoch (J2000.0); the mean CCD observational position is not published. The level of completeness (about 80%) is the same for UCAC1 and UCAC2, avoiding all “problem cases” such as elongated images and blended images of close double stars. For the final release (UCAC3) likely both the mean observational data and the “best” compiled positions and proper motions will be published, with major improvements in completeness.

## 2. OBSERVATIONS

Improvements in data for UCAC2 over UCAC1 fall into 2 categories: current epoch observations with the astrograph and new measurements of early epoch photographic plates. Remeasurements of early epoch plates have been undertaken of 2 different sets with 2 different machines as described in Section 4 (proper motions).

Table 1 gives an overview about the Twin Astrograph, its camera and data acquisition. Table 2 lists some achieved and expected milestones of the

UCAC project. All observing is performed with guided exposures (no drift scanning). The red-corrected lens of the Twin Astrograph is used for the survey imaging while the visual-corrected lens carries the ST-4 autoguider. Operation is semi-automatic with some supervision by an observer. For more details about the instrument, observing procedure, and quality control, the reader is referred to Paper I.

A break in the observing occurred in September/October 2001 when the astrograph was disassembled at Cerro Tololo, shipped to Arizona and assembled at NOFS. Test observations after assembly indicated no significant tilt of the detector w.r.t. the focal plane and regular survey observing continued after only 42 nights of down time due to the relocation. Regular observing at CTIO had the astrograph on the west side of the pier, while at NOFS it is on the east.

As part of the UCAC project, fields with optical counterparts of International Celestial Reference Frame (ICRF) sources are being observed (about 4 times per year) at larger telescopes to provide a direct link to the extragalactic reference frame. Contemporaneous to these observing runs at the larger telescopes the same fields are observed at the astrograph. These special observations ( $\approx 10$  to 16 CCD frames per field) are in addition to the regular survey observations and are taken with the astrograph on the east and west of the pier. Neither these special astrograph data nor the deep field data were used for UCAC2. A separate paper describing these observations and results is in preparation (Zacharias et al. 2004).

## 3. CURRENT EPOCH POSITIONS

This section describes the reduction procedures applied to the CCD astrograph observations in order to derive mean observed positions at the current epoch. The same general procedure steps were followed as for UCAC1 (see Paper I); however, the modelling of systematic errors is now performed on a more sophisticated level, as will be discussed in the following sections.

### 3.1. From pixel to $x, y$

Exactly the same procedures as for UCAC1 were applied for the UCAC2 raw data reductions. Dark frames of the same exposure time as the ob-

ject frames were applied to the raw CCD frames, but without any flat corrections. A 2-dimensional Gaussian model was used for the image profile fits, resulting in the same raw  $x, y$  data as for UCAC1, using the same software (Winter 1999). A re-processing of the entire pixel data with improved models, including double star fits, will be attempted for the final UCAC release.

### 3.2. Pixel Phase

As described in Paper I, a position derived from undersampled pixel data of a stellar image has a systematic error as a function of location of the image centroid with respect to the pixel boundaries (pixel phase), whenever the fit model profile function does not perfectly match the data. The systematic error in the derived position (per coordinate) follows approximately a sine-curve as a function of the pixel phase. An empirical function was derived in Paper I based on the reference star residuals from all applicable CCD frames used for UCAC1. An amplitude of order 12 mas was found for this effect and the UCAC1 data were corrected globally for all individual  $x, y$  centroid positions accordingly.

For UCAC2 this systematic error was further investigated as a function of the undersampling, i.e., the width of the image profiles, which vary with seeing conditions. The observational data were split into 4 groups by mean full width at half maximum (FWHM) of images of CCD frames, as obtained from the quality control pipeline. Each group showed the familiar sine-curve for systematic errors in position as a function of the pixel phase. However, the amplitude of that function also shows a clear dependence on the FWHM. These results were interpolated and a look-up table with corrections was generated. Figure 1 shows a graphical representation of it. For UCAC2, image centroid positions were corrected accordingly, as a function of pixel phase (individual image) and FWHM of image profiles (mean of each CCD frame).

### 3.3. CTE Effect

The 4k CCD chip in our astrograph camera has a relatively poor charge transfer efficiency (CTE). This leads to a coma-like systematic error in the uncorrected stellar positions mainly along the  $x$ -

axis (right ascension), which is the direction of fast clocking of charge. The  $y$ -axis is affected as well; however, to a much lesser degree due to the slower clocking of charge in that direction. A simple, empirical model has been used for corrections of UCAC1 positions. For the UCAC2 we extended that model, which remains an empirical approach in correcting derived  $x, y$  positions.

The poor CTE leads to asymmetric images. The degree of asymmetry increases from nothing (near  $x = 0$ ) to the maximum effect near  $x = 4094$  pixel. The stellar image profiles are fitted with a symmetric, Gaussian function. This results in a systematic error of the centroid positions as a function of various parameters like brightness of the star and profile width, always coupled with a function of  $x$ . Using a non-symmetric model function for astrometry leads to an ambiguous definition of "centroid" (becoming a function of various parameters), thus the problem is just redefined without being solved. Initial tests with "fixing" the pixel data itself were not successful. The centroid position of (critically sampled) image profiles is very sensitive to manipulations of pixel counts. This issue will be readdressed in the final UCAC reductions.

Empirical corrections (in the  $x, y$  domain) for this CTE effect can be derived by comparing CCD images taken of the same field but with the telescope flipped w.r.t. the sky by  $180^\circ$ . However, there is a degeneracy with a pure magnitude equation term. This degeneracy can be resolved by additional observations of overlapping fields. More observations of calibration fields along these lines are in progress; however, results will not be included until the final UCAC release. As with UCAC1, corrections for UCAC2 positions derived from the flip observations are interpreted as magnitude times coordinate effects. Deriving such corrections from the  $x, y$ -data has the advantage of a strong statistic, utilizing thousands of stellar positions in a given frame. The much sparser reference star residuals have been used as an external check showing only very small, pure magnitude-dependent systematic errors (see Section 3.6), thus confirming our assumption.

For the UCAC2 data a more sophisticated model than for UCAC1 has been derived from the flip observations of dense calibration fields. Position corrections ( $\Delta x, \Delta y$ ) for individual stellar im-

age centroids ( $x, y = 0$  to 4,094 pixel) were applied because of the low CTE as a function of  $x, y$ , and relative instrumental magnitude ( $m \approx -3... + 3$  mag) according to

$$\Delta x = c_1 m x + c_2 m^2 x + c_3 m^3 x + c_4 m x^2$$

$$\Delta y = d_1 m y + d_2 m^2 y + d_3 m^3 y + d_4 m y^2$$

The parameters  $c_1$  through  $d_4$  are found to be a function of exposure time ( $t$ ) and mean image profile width ( $FWHM$ ) of a CCD frame. The mean parameters are summarized in Table 3, and the modifying factors  $k$  as a function of  $FWHM$  are given in Table 4. Note,  $k$  is different for long ( $\geq 70$  sec) and short exposure frames. The  $c$  and  $d$  coefficients in the above equations are formed by the product of the  $c, d$  values in Table 3 with the  $k$  factors in Table 4.

The corrections for the  $y$ -coordinate are smaller than for the  $x$ -axis, but nevertheless are significant and have been applied to all UCAC2 positions. Typical corrections for the CTE effect are up to about 25 mas and 10 mas for large  $x$  and  $y$  pixel coordinates, respectively. UCAC1 positions were corrected only for  $x$  and only using the first-order term.

The CTE effect furthermore varies as a function of background illumination (phase of the Moon and distance of observed field to the Moon). Special calibration observations are being taken and will be considered in the final UCAC release. Observations with the camera rotated by  $90^\circ$  and  $270^\circ$  were made at the beginning of the project and are also planned for after the completion of the regular survey. These data will aid in determining corrections to systematic errors as well.

### 3.4. Near Saturation

There are systematic errors in the  $x, y$  positions of bright stellar images. Similar to UCAC1, empirical corrections were derived from the reference star residuals as a function of the image profile amplitude. Nominal saturation is around an amplitude of 15,000 counts. The corrections applied to the UCAC2 observed positions are summarized in Table 5. These numbers are slightly updated w.r.t. the UCAC1 solution, based on more data and in the context of other changes in systematic

error corrections; however, no new procedures or models were introduced here. Images close to saturation should be used with care. Even after applying these systematic corrections, the positional errors of such overexposed stars are larger than for well exposed stars. Estimated positional errors for individual stars are presented in the catalog based on the scatter of individual images.

### 3.5. Field Distortions

Systematic errors of star positions depending on the location in the focal plane ( $x, y$ ) have been derived by binning the reference star residuals from thousands of individual CCD frames, following the procedures outlined in Paper I. Separate field distortion patterns (FDP) were generated for the data taken at CTIO and NOFS (Figure 2 and 3). The split of data was necessary because the telescope was disassembled and reassembled between the locations, which likely changed some parameters slightly like tilt of the focal plane. Also, all survey observing at CTIO was performed with the telescope on the west side of the pier, while at NOFS the telescope is on the east for regular observing.

### 3.6. Individual Positions

The subset of astrometrically “good” stars (no indication of multiplicity) from the Tycho-2 catalog (Høg et al. 2000) were used as reference stars for the astrograph CCD frames. This represents on average a 2.5-fold increase in the number of reference stars available as compared to the UCAC1 reductions (mainly based on the ACT (Urban et al. 1998), thus the original Tycho stars). After correcting the  $x, y$  pixel data for the above mentioned effects, a linear plate model was used for the individual CCD frames.

Apparent places and refraction were handled rigorously in a weighted adjustment, considering errors of the reference star positions at the epoch of observations, formal  $x, y$  fit errors and a contribution from the atmospheric turbulence (as a function of the exposure time; 20 mas for 100 sec; scaled by  $t^{-1/2}$ ). Images with an amplitude over 14,500 counts were downweighted with an additional root-sum-square (RSS) error of 60 mas. Outliers (3-sigma) were removed and the reductions repeated if necessary. The largest residual

was removed and the reduction repeated whenever the adjustment error exceeded 1.5 times the expected mean error of unit weight. A total of 156,280 and 28,416 frames taken at CTIO and NOFS, respectively, were used, providing over 10 million residuals per coordinate. This gives about 55 reference stars per CCD frame on average.

Figure 4 and 5 show examples of the residuals from the CTIO data as a function of  $x, y$  coordinates, magnitude, amplitude, and color index, separately for the long and short exposures. There are still some systematic effects visible; however, they are on the 5 mas level, becoming visible here only due to the extreme binning of 3,000 residuals per plot point. Results for the data taken at NOFS are similar.

### 3.7. Comparison of Data Taken at CTIO and NOFS

The last  $\approx 130$  fields (near  $+25^\circ$  declination) observed at CTIO were repeated immediately after relocation of the CCD astrograph to NOFS. Although reduced with the same reference stars, the 2 sets have a variety of different properties. The fields were taken with the telescope flipped in orientation and different field distortion corrections were applied. The zenith distances of the sets are about  $55^\circ$  and  $10^\circ$  respectively. The average seeing conditions were better at CTIO than at NOFS.

Figure 6 and 7 show results from a comparison of 144,480 star positions in common as observed from CTIO and NOFS. This gives an indication about remaining systematic errors after going through the reduction pipeline as described above. Systematic differences are typically below the 10 mas level. The precision of positions from each set (CTIO or NOFS) is the RMS value in Figure 7 divided by  $\sqrt{2}$ , assuming equal errors for both sets. This is about  $30 / \sqrt{2}$  mas  $\approx 20$  mas for  $R = 13^m$  stars, of which all are field stars (non-reference stars).

### 3.8. Mean Positions

Individual positions from the CCD frame reductions were combined to mean, weighted positions, assuming a match radius of 1 arcsec. Only sources with at least 2 images were retained. Different entries within 3 arcsec were removed entirely from

the mean position file to avoid problems with close double stars and spurious detections around over-exposure features. Entries with a formal position error of over 200 mas in either coordinate were excluded as well.

A total of 58,728,437 star positions were obtained for observing epochs from 1998.1 to 2002.9. The mean, formal position error is about 30 mas per coordinate and is a function of magnitude (Figure 8). The precision for 10 to 14 magnitude stars is about 15 to 25 mas, increasing to 70 mas at  $R = 16$ .

Based on the reference star residuals (see Fig. 4), a slight magnitude equation correction was applied to the final positions ( $-2$  to  $+8$  mas, almost linear for 9th to 12.5th magnitude, then flat for all fainter magnitudes). This also reduced the differences between the UCAC1 and UCAC2 positions systematically.

## 4. PROPER MOTIONS

The proper motions and their error estimates of the UCAC2 stars were compiled in a manner similar to UCAC1. Weights were used from formal catalog errors. For the YS3 data (see below) a random error of 150 mas per coordinate was assumed. For the astrograph data, formal errors of individual star positions were used with a minimum value of 15 mas per coordinate in order to not create an artificially high weight due to small number statistics. For more details readers should refer to Paper I.

UCAC2 encompasses 2 new data sets that greatly improve the proper motions. For the stars fainter than  $V \approx 12.5$ , instead of the USNO-A2.0 data being used as in UCAC1, the Yellow Sky 3.0 (YS3) catalog was used. The YS3 data are from astrographs and are of better quality than the USNO-A2.0, derived from Schmidt plate data. The second major new data set was from recent measure of the AGK2 plates, on loan to USNO from the Hamburg Observatory.

### 4.1. Yellow Sky 3.0

#### 4.1.1. Plate data

The Yellow Sky 3.0 (YS3) catalog was compiled from measures made by the US Naval Observatory's Precision Measuring Machine (PMM;

Monet et al., 2003) of the second epoch yellow plates taken as part of the Northern Proper Motion Survey (NPM; Klemola et al., 1987) and first epoch yellow plates taken as part of the Yale/San Juan Southern Proper Motion Survey (SPM; Platais et al., 1998). Due to the incompleteness of the SPM, the 1,246 NPM plates with field centers of  $\delta \geq -20^\circ$  were used in conjunction with the 598 SPM plates with field centers  $\delta \leq -25^\circ$ . The NPM plate epochs range from 1969 to 1988 with a median value of 1976, and the SPM plate epochs range from 1965 to 1974 with a median value of 1969. Each plate contains a long (2 hour) and short (2 min) exposure, called System-I and System-II, respectively. A wire grating was used in front of the lens which produces diffraction images of bright stars (attenuation of about 4 magnitudes). The central image (for faint and bright stars) is called 0th order. For bright stars higher order images are visible symmetrically around the central image.

#### 4.1.2. Initial catalog

Extensive analysis indicated that the System-I 0th order images were just coming out of saturation at the faintest magnitudes included in the Tycho-2 catalog. Hence, the astrometric reduction was based on the preparation of a plate-by-plate catalog of Tycho-2 stars fainter than  $V = 12$ , and the correlation of this catalog with the measures from the PMM. Included in the correlation, but given zero astrometric weight, were measures taken from the USNO-A2.0 catalog. Given the very confused nature of the NPM and SPM plates (System-I and -II images and the various orders from the objective grating), only PMM measures that could be correlated with an external catalog were included in the YS3 catalog. In this way, a reasonably complete catalog could be compiled down to the plate limit (about  $V = 18$ ). The PMM's accuracy is believed to be in the range of 100 mas, but the YS3 reduction errors are dominated by unmodeled systematic errors.

During the reductions of the Yellow Sky data, the grating images were used to minimize systematic errors by magnitude. This was not entirely successful, as shown in the next section. One possible explanation is that the grating images have a different image profile than fainter, non-grated images. In order for these errors – and other sys-

tematic errors such as those as a function of the  $x, y$  location of an image on a plate – not to propagate into the proper motion system of the UCAC2, they were further investigated and minimized.

#### 4.1.3. Field distortion pattern

Under close examination using Tycho-2, UCAC, and 2MASS astrometry, systematic deviations as a function of star location on a plate (measured  $x, y$  values), survey (NPM or SPM), and magnitude range were found. These were treated similarly to the field distortion pattern (FDP) of the astrophotograph data (Section 3.5) and their removal was handled in a similar fashion. Briefly, the FDP is removed by using a mask that is determined by averaging residuals within 4,096 individual bins (64x64 across the  $x, y$  field). Each bin contains data from stars from the same survey and with similar magnitudes. The magnitude ranges used are based on the rapidity with which the FDP changes and the desire to use at least 200,000 stars per mask. To minimize rapid fluctuations from bin to bin, the data were smoothed. The end result is the minimizing of the systematic errors on the individual plate level. As an example, Figure 9 shows the FDP for all Tycho-2 stars of the NPM data set before corrections. The equivalent figure for the SPM data set show a similar pattern; however, the differences are in the opposite sense and are roughly 1.5 times larger. After applying the FDP corrections, the mean residual vectors are zero.

#### 4.1.4. SPM, NPM discontinuity

On a global level, the original YS3 shows a discontinuity between the NPM and SPM surveys of between 150 and 200 mas. This is most strikingly seen in the differences in declination as a function of declination, as shown in Figure 10. (Due to the plate overlap pattern and the fact that the NPM/SPM surveys are separated along a declination boundary, any right ascension band will have stars from all  $x, y$  measures and both surveys. Thus plots of the the differences as a function of right ascension do not clearly show this type of discontinuity.) This effect is only present in the non-Tycho-2 stars (top diagram in Fig. 10). The reasons for this are not quite clear; it is not entirely due to the epoch difference between the Northern and Southern surveys, although this accounts

for some of the apparent discontinuity. Unfortunately, there is not a high quality reference catalog available in the magnitudes fainter than Tycho-2 that can be utilized. To minimize the discontinuity, a YS3 minus Tycho-2 average difference in RA and Dec on each plate is determined, using the epoch 2000 position (no proper motion applied). If enough stars are available to eliminate the random proper motion, then the averages correspond to the proper motion as seen solely due to solar motion plus galactic rotation toward the direction of the plate center (given the set of stars). The middle diagram in Figure 10 shows this. High proper motion stars, which are typically in close proximity to the Sun, are not used. Next, the YS3 and non-Tycho-2 stars are differenced and averaged in the same way. On the premise that the Tycho-2 stars and the non-Tycho-2 stars are at similar distances, then the difference between these values should be near zero. Application of their difference to the non-Tycho-2 stars was performed, and most of the discontinuity between the two surveys disappeared, as seen in Figure 10 (bottom).

The authors understand that the above mentioned method is not without problems, but it will reduce a plate zero-point error where one exists. Since it is fundamentally based on an extrapolation by magnitude, it may result in an over- or under-correction which is virtually impossible to discover. These corrections, if significantly wrong for the fainter stars, would impart a systematic error by magnitude that would propagate into the UCAC2 proper motions. This would render the UCAC2 dangerous to use for some studies, especially when comparing data sets that include both Tycho-2 stars and the fainter set. The authors have weighed this carefully, and believe that keeping the discontinuity in the YS3 dataset is more harmful.

In Figure 10, a “sawtooth” pattern in the SPM data is seen. Although it appears to be a function of star location on a plate, the corrected FDP plots do not show it. Several attempts to uncover the cause and correct it have been tried, all without success. It remains in the data and therefore in the proper motions. With a 50 mas systematic error at the epoch of the SPM plates, one can expect this to lead to 1-2 mas/yr systematic error in the proper motions. Since it appears to be a function of plate location, users are warned that

systematic errors of this size are likely over an area of a few degrees. Some results discussed in Section 5.3 relate directly to these zero-point corrections. A new reduction of the NPM and SPM plates utilizing both the yellow and the blue plate data has been completed, but not in time to be incorporated into the UCAC2 proper motions. This will be discussed in a future paper.

## 4.2. AGK2

### 4.2.1. Plate data

Between 1928 and 1931 the sky north of declination  $-5^\circ$  was photographed on 1940 glass plates each covering over 5 by 5 degrees with two dedicated astrographs located in Bonn and Hamburg, Germany. The astrographs were of similar design; each had a 4-lens system with 0.15 m aperture and focal length of 2.0 meters leading to a plate scale of 100 arcsec/mm. Data from both instruments were kept uniform. Two exposures, one of 3 minutes and one of 10 minutes, were made on each plate. The plates were taken in a corner-in-center pattern, so each area of sky was photographed on two plates. The emulsion used was fine grain and blue sensitive. Magnitude ranges for the measurable stars are from  $B \approx 4$  to 12. During the 1930s, 1940s and 1950s, the measuring and reduction of the brighter stars were carried out by hand. The resulting catalog, called “Zweiter Katalog der Astronomischen Gesellschaft,” AGK2 (Schorr & Kohlschutter, 1951), contains about 186,000 stars with positional accuracies of about 200 mas at the observational epoch. However,  $\approx 10$  times more stars are measurable on the plates. Additionally, the inherent accuracies from the plate data for a well exposed images are  $\approx 100$  mas; hence, if good reductions can be made and systematic errors can be handled, positions good from 50 to 70 mas (due to two exposures and the overlapping plate pattern) can be achieved. This combination of early epoch and high achievable positional accuracies makes the AGK2 plates a source of highly accurate proper motions ( $\approx 1$  mas/yr) for about 2 million stars.

### 4.2.2. Remeasures

The AGK2 plates were properly stored at Hamburg Observatory for the last  $\approx 70$  years and are still in excellent condition. In 2001, the Hamburg

Observatory loaned all AGK2 plates to USNO for remeasurement. The USNO StarScan machine in Washington DC started to measure those plates in early 2002; measuring was completed by March, 2003. This machine has a large granite stage, 0.1  $\mu\text{m}$  stage encoders, a temperature-controlled room and automatic plate clamping and rotation. All images on all plates are digitized in two orientations using a CCD camera behind a telecentric lens. A two-dimensional Gaussian fit to the images is made, and care is taken to remove systematic errors arising from the lens system and measuring machine. The repeatability of the StarScan machine is  $\approx 0.2 \mu\text{m}$  and measurements are accurate to at least  $0.5 \mu\text{m}$ .

#### 4.2.3. Reductions

The data comprising the HCRF (IAU 2000), that is the Hipparcos stars without a Double and Multiple System Annex flag, are used exclusively for plate reductions. During the reduction process, it was determined that the Bonn plates (centered at declinations  $2.5^\circ$  to  $+20^\circ$ ) had a large systematic error by color that needed further investigation, so it was decided not to include these in the UCAC2. Only data from from the Hamburg plates (centered at declinations north of  $+20^\circ$ ) were used. The entire set of plates, both Hamburg and Bonn, will be used in the final UCAC catalog, slated for 2005.

Preliminary positions have been obtained for over 950,000 stars from a subset of 869 of the Hamburg plates; 599,871 of these positions were used for the UCAC2 proper motions. All areas north of  $+20^\circ$  covered by the UCAC2 are included. Although considered preliminary until the final AGK2 re-measurement catalog is completed in 2004, the data are high-quality. For well-exposed images, positional errors of  $\approx 70$  mas per star coordinate are obtained. With the  $\approx 70$  year epoch difference between that and the UCAC observations, proper motions good to 1 mas/yr are obtained. This is a factor of  $\approx 2$  better than previously best known (from AC2000 minus Tycho-2) for stars in this magnitude range and comparable to the better Hipparcos stars.

On average there are about 50 Hipparcos reference stars per plate. For the reference stars used here, the average error in Hipparcos proper motions is 1.3 and 1.1 mas/yr for the RA and

Dec component, respectively. This gives an expected, average Hipparcos position error for the 1930 epoch of about 72 mas per coordinate, which is similar to the  $x, y$  errors. Each of the 2 exposures per plate was reduced separately. A field distortion pattern was generated from preliminary reductions and applied to the  $x, y$  data, which takes care of the small but significant 3rd order optical distortion of the lens; and other effects.

#### 4.2.4. Results

Figure 11 shows the binned residuals as a function of magnitude, coma term, and color of preliminary AGK2 reductions. Significant magnitude- and color-dependent terms are obvious. The data were corrected for an average coma-term in both coordinates, using the measured magnitude for all stars.

Systematic errors as a function of color are summarized in Table 6. These have been taken out for the Hipparcos stars, but corrections for all field stars are not possible due to the lack of color information. Thus the positions for field stars here assume a mean color index of about  $(B-V) = 0.8$ . A significant color magnification error was found and the  $x, y$  data were corrected as a function of relative color index times radial distance of images from the plate center. This is correct only for the reference stars, where a color index was available. For field stars we again assume here a mean color index of about  $(B-V) = 0.8$  (zero point of corrections).

For the AGK2 plate reductions for the UCAC2 release, a 10-parameter plate model (total for  $x$  and  $y$  coordinates) was adopted, including 6 linear, 2 plate tilt terms and a linear magnitude equation term per coordinate. The use of magnitude terms is reasonable because the full magnitude range of the  $x, y$  data is covered by the reference stars and the density and accuracy of the reference stars is sufficient. Magnitude parameters are significant at the 2-sigma level for individual plates. Dropping the magnitude equation terms from the plate reductions and applying a mean correction gave slightly inferior results.

The plates of the Bonn zone showed even larger systematic errors, mainly as a function of color (see Table 6), and could not be reduced properly within the timeline of UCAC2. The full AGK2

material will be used in the final version of the UCAC, after color information for most AGK2 stars have been identified.

Formal standard errors for mean AGK2 positions are in the range of 40 to 80 mas when 4 images were available (2 plates, 2 exposures), with a mean of 51 mas. In case of only 2 images per star, the range is about 40 to 150 mas, with a mean of 115 mas.

## 5. EXTERNAL COMPARISONS

### 5.1. 2MASS positions

The UCAC2 has been compared with the 2MASS all-sky infrared catalog (Cutri et al. 2003), which was released in spring 2003. For details of this comparison see Zacharias et al. (2003). The 2MASS was observed between 1997 and 2001, providing J, H, and  $K_S$  magnitudes and precise positions on the HCRF (also via Tycho-2 reference stars) for over 470 million stars, covering the entire UCAC2 sky area and magnitude range.

Systematic differences between UCAC2 and 2MASS positions are only at the 5 to 10 mas level. Position differences as a function of UCAC magnitude for 2 declination zones are shown in Figure 12 as typical examples. The UCAC2 proper motions were used to bring the UCAC2 positions to the 2MASS observational epoch for individual stars. For the  $R = 11$  to 14 mag range, the UCAC2 positional errors are negligible in this comparison, revealing an external positional error of 2MASS positions of about 70 mas. It is reasonable to assume that 2MASS positional errors (due to low S/N) start to increase only beyond  $R = 16$ , thus providing an external estimate for UCAC2 positional errors at its limiting magnitude, confirming the internal estimates. Systematic differences (UCAC–2MASS) as a function of color are insignificant ( $\leq 5$  mas).

### 5.2. Other Positional Comparisons

UCAC2 was also compared with the CMC13 (Evans et al. 2003), the M2000 (Rapaport et al. 2001) and ACR (Stone et al. 1999). All these catalogs cover the 10 to 16 magnitude range of UCAC2, but only in certain declination zones. UCAC2 systematically agrees with CMC13 and M2000 within 10 to 20 mas, while a significant

magnitude equation is found in the ACR data (up to 50 mas w.r.t. the other catalogs). Random positional errors of UCAC2 are confirmed to be about 15 to 25 mas for  $R \approx 10$  to 14, increasing to 70 mas at  $R = 16$ . For a detailed comparison see Evans et al. (2004).

### 5.3. Proper Motion Comparisons

In order to estimate the accuracy of the UCAC2 proper motions, various external comparisons were performed. The match of 2QZ and SDSS quasars with UCAC2 turned up only 1 and 4 sources in common, respectively, with UCAC2 proper motion offsets consistent with zero within formal errors. Too many objects listed as “galaxy” in the SDSS data turned out to be overexposed stars. Saturation is around 15th magnitude in SDSS which does not leave much overlap with UCAC2 data and no reliable comparison could be made.

Results of 3 cases with significant statistics are summarized in Table 7. In all cases the results depend slightly on the cut for outliers. Here a 3-sigma limit has been used. For the Large Magellanic Cloud (LMC) stars (line 1 in Table 7), a true proper motion of +1.94 and  $-0.14$  mas/yr for the RA and Dec. component, respectively, was assumed (Kroupa & Bastian 1997). Similar to Paper I, the SPM (manually confirmed) galaxies were used (line 2 in Table 7) as well.

The ERLcat data (de Vegt et al. 2001) provides positions from the Hamburg Zone Astrograph and the USNO Black Birch Astrograph programs derived from photographic plates (V band-pass) of epochs mainly between 1980 and 1992. Only Hipparcos stars were used as reference stars. ERLcat stars are located in 1 square degree fields around about 350 ICRF sources all over the sky. Proper motions from ERLcat data were derived by combining these V-band positions with UCAC2 (J2000) positions. Comparisons were then made to the UCAC2 proper motions, which do not include the ERLcat data. This is basically a comparison between the ERLcat and Yellow Sky data. Formal errors for individual ERLcat proper motions were also calculated. Stars with a difference in proper motion outside 3-sigma were rejected for this statistic. Excluding or including stars brighter than  $V = 11.5$  (Tycho-2 stars) did not affect the results.

Table 8 shows proper motion comparisons UCAC2–ERLcat as a function of declination zones. The  $-90^\circ$  to  $-60^\circ$  declination zone shows large differences and has been excluded from the mean statistics. A plot of  $\Delta\mu_{\alpha \cos \delta}$  versus  $\alpha$  shows a  $\pm 15$  mas wave signature. All other areas in the sky show consistent proper motions with mean differences  $\leq 1$  mas/yr, and local differences (average over stars of a single ICRF field) of up to  $\pm 4$  mas/yr. With the short baseline of only about 10 years for the ERLcat proper motions, this translates to positional offsets of about 40 mas, which is expected for some of the ERLcat fields when assuming a reasonable 1-sigma = 20 to 30 mas zero-point error for the positions of the ERLcat fields. Systematic errors of similar magnitude are also possible in the YS3 data, as Figure 10 indicates.

In summary, a systematic error of the UCAC2 proper motions of about 0.5 to 1.0 mas/yr per coordinate can be expected. Most of the UCAC2 proper motions are 2 position proper motions, derived from the Yellow Sky data as early epoch. With an average 30 years of epoch difference, this translates to about 15 to 30 mas systematic error in the YS data, which is very reasonable.

The observed scatter of the proper motions in these sets are generally larger than the internal, formal, mean errors given for the UCAC2 proper motions by a factor of 1.1 to 1.5. The larger values apply for the galaxies.

## 6. THE CATALOG

### 6.1. Overview

Contrary to UCAC1, which was an observational catalog, UCAC2 is a compiled catalog. Positions and proper motions are given for the standard epoch of J2000.0, on the Hipparcos system (HCRF, ICRS). UCAC1 is now superseded by UCAC2, with the following major advantages: much larger sky coverage, improved systematic error corrections, addition of large, new early epoch catalogs for improved proper motions, and inclusion of accurate 2MASS photometry.

Figure 13 shows the sky coverage of the UCAC2 as observed from the NOFS location. The entire sky area south of the band shown was completed at CTIO prior to the relocation of the telescope. Thus Figure 13 shows the border between CTIO

and NOFS data as well as the overall sky completeness limit for data included in this release. Various sky coverage color plots are presented at our Web page (<http://ad.usno.navy.mil/ucac>) and on the CDs.

Figure 8 shows the formal, standard errors of UCAC2 positions at the mean CCD astrograph observing epoch as a function of magnitude. Figure 14 shows the formal, standard errors of UCAC2 proper motions as a function of magnitude, separately for the northern and southern hemisphere. There are no significant differences between the RA and Dec component (not shown here). However, the proper motions for the northern hemisphere are consistently better than for the south (slightly earlier epoch of NPM than SPM data). The largest improvement is seen for the 10th to 12th magnitude stars, caused by the inclusion of AGK2 data for a large section of the northern hemisphere.

### 6.2. Data Representation

The UCAC2 is distributed on 3 CDs. Each CD contains an introduction, sample files, and access software. The data are arranged in zones of half a degree width in declination. The zone files 1 to 106 ( $-90^\circ$  to  $-37^\circ$ ) are on CD1, followed by zone files 107 to 182 ( $+1^\circ$ ) on CD2, and the most northern part on CD3, up to zone 288 ( $+54^\circ$ ). Sources on each such file are sorted by right ascension. For each source there is a binary record of 44 bytes length with byte order for an Intel processor. The provided access software (Fortran) checks for a byte-flip, and applies it if needed. Table 9 explains the data content and format for each source record, while Table 10 gives an example for the first 5 stars of zone 1. There are no blank entries; however, “no data” is represented by some out-of-range numbers, as explained in the notes.

Sources in UCAC2 can be identified by giving reference to their position or using the UCAC2 identification number (8 digits, preceded by the string “2UCAC”). UCAC is an acronym registered with the IAU task group of designations. The ID number is a running number over all entries, which is generated by the access software or can be calculated by the user as described in the “readme.txt” file. This option for naming sources is also supported by the IAU and is very convenient for indexing in cross-referencing. The

UCAC1 identification numbers are different than the UCAC2 numbers, and the final release will have new IDs as well.

### 6.3. Important Notes

The user is urged to read the “readme.txt” file available on each CD as well as at our UCAC Web page (<http://ad.usno.navy.mil/ucac/>). It provides important notes to the data, and explains the flags and limitations of the catalog. A few important items are mentioned here.

#### 6.3.1. Completeness

UCAC2 is not complete, even in the sky area covered. Bright, overexposed stars are excluded. UCAC2 is not complete at 8th magnitude or brighter. The UCAC team is currently working on a bright star supplement (Urban et al. 2004) to the UCAC2, which will include Hipparcos and Tycho-2 astrometry for those bright stars not in the UCAC2 observational data. All “problem cases” (multiples, outliers) are excluded during the reduction procedures. Only sources detected on at least 2 astrograph CCD frames are included. Double stars with separations in the 0.5 to 5 arcsec range are likely not in UCAC2, with detected multiple entries within 3 arcsec explicitly excluded. About 15% of the astrograph mean position entries were dropped for the UCAC2 release due to missing, unique matches with an earlier epoch catalog. All entries in the published UCAC2 have a proper motion.

#### 6.3.2. Magnitudes

Accurate infrared photometry is provided from the 2MASS project; however, only the basic information per star is copied into UCAC2. The astrograph red-magnitudes (579–642 nm bandpass) are very crude and provided for identification purposes. These magnitudes are obtained from image profile fits and are not aperture photometry (flux) results. Observations often continued in non-photometric conditions and systematic errors of these magnitudes as a function of magnitude and  $x$ -pixel location are expected due to the CTE problem of the CCD (see Section 3.3) and the mismatch of data and fit-model image profiles. Locally (sky area, magnitude range) these

red-magnitudes have an expected error of about 0.1 mag with an absolute error of  $\approx 0.3$  mag.

#### 6.3.3. High proper motion stars

There are 18,604 previously known high proper motion stars in the UCAC2 observational position file. These were identified by Gould and Salim (private comm.) utilizing the NLTT Catalog and graciously forwarded to the UCAC team. However, only those high proper motion stars with an early epoch, astrometric position available were included. There were 8,282 stars found in our standard catalogs (Yellow Sky, AC 2000.2, Tycho-2, Hipparcos, other transit circle and photographic catalogs), while 7,666 stars were supplemented utilizing positions from the USNO A2; thus, a total of 15,948 NLTT stars are in the UCAC2. Note that these are the only stars for which the USNO A2 is utilized, as we are trying to minimize the reliance on Schmidt plate data in the UCAC2.

#### 6.3.4. Non-stellar sources

The UCAC2 contains some galaxies, particularly at the faint end. No flag indicating a galaxy or star is provided with this release; however, extended objects are very unlikely to be in the UCAC2 due to the detection and reduction quality control procedures adopted for the catalog construction. Also, galaxies of integrated magnitudes of  $\approx 15$  or fainter are likely to show cores fainter than 16th magnitude and, thus, will likely not be in the UCAC2.

A few asteroids might be hidden in the UCAC2. The observing schedule actively avoided all major planets and bright asteroids (to 12th mag). However, asteroids in the  $\approx 12$  to 14 mag range can appear on both the long and short exposure taken within 2 minutes and could give a satisfactory position match. Fainter asteroids could enter the UCAC2 only if overlapping fields with the object were taken within a short period of time. Additionally, with the requirement that each object has a proper motion using an early epoch catalog, it is unlikely that many asteroids are present in the UCAC2.

## 7. DISCUSSIONS AND CONCLUSIONS

UCAC2 provides the most accurate positions and proper motions available today for most of

the stars in the 9th to 16th magnitude range and the 86% of the sky covered so far. External, random errors are close to the quoted, internal errors. The 2MASS infrared photometry added to the data will be of benefit for the user, particularly for stellar statistics and galactic kinematics investigations. The average error of proper motions for the  $R = 13$  to 16 magnitude stars is about 6 mas/yr, dramatically improved over the UCAC1, thanks to the inclusion of the Yellow Sky catalog. For brighter stars, with the inclusion of Hipparcos, Tycho, AGK2 and all catalogs used for the Tycho-2 construction, proper motion errors in the 1 to 2 mas/yr range could be achieved.

The high positional accuracy of UCAC at current epoch has been exploited in the minor planet community and has proven essential for occultation predictions (Dunham 2004)<sup>1</sup>. The goal, providing a densification of reference stars beyond the Hipparcos / Tycho-2 catalogs, has been achieved. The average density of UCAC2 is 1,360 stars per square degree, with a positional accuracy of stars to 14th magnitude close to the current epoch position errors of the Hipparcos Catalogue.

For most applications UCAC2 supersedes even Tycho-2 in the sky area covered for stars fainter than about 9th magnitude. However, UCAC2 is limited by remaining systematic errors on the 5 to 10 mas level, which – although very small – is significantly worse than for the Hipparcos Catalogue. Systematic errors in the UCAC2 proper motions have not been investigated in great detail yet. Comparisons with identified very distant sources indicate no obvious problem, with expected systematic errors on the 1 mas/yr level.

Using UCAC2 for determining a possible system offset (rotation) between HCRF and ICRF at current epochs via observations of counterparts of extragalactic radio sources is severely limited by the remaining systematic errors in UCAC2 positions. To overcome this, as part of the UCAC project, these sources are observed with deep CCD images. The same fields are simultaneously observed with the UCAC astrograph on the east and west of the pier. These special observations are not included in the UCAC2 release. Mean positions derived from these additional observations

<sup>1</sup>see also <http://www.asteroidoccultation.com> and <http://mpocc.astro.cz>

will have much smaller systematic errors.

One more final data release of UCAC is planned after the completion of the all-sky survey. It is envisioned that the pixel data will be re-processed for UCAC3, which should slightly improve the astrometric accuracy. The main advantage will be a completeness level to over 99%, thus providing accurate positions for many known and new double stars. The astrograph could be used for future projects (Zacharias 2003); however, a bigger telescope is required to make significant progress in further densification efforts. USNO has plans for a dedicated, astrometric, robotic, wide-field telescope for an all-sky survey to about 20th magnitude with positions on the 5 to 10 mas level to  $R = 18^m$  (de Vegt, Laux & Zacharias 2003).

We are grateful to the observers D. Castillo, M. Martinez, and S. Pizarro (CTIO), T. Tilleman, S. Potter, and D. Marcello (NOFS). We thank the CTIO staff; in particular O. Saa and the director M. Smith, the NOFS staff in particular M. Divittorio, B. Canzian, and C. Dahn, and the USNO Washington instrument shop, in particular G. Wieder and J. Pohlman. E. Holdenried and G. Hennessy are thanked for system software support. M. Germain, S. Gauss, T. Corbin, and K. Seidelmann are thanked for their effort and support in getting the project going. Spectral Instruments, in particular G. Sims, is thanked for the outstanding support of our camera. R. Stiening (Univ. of Massachusetts) is thanked for providing 2MASS data at various stages of the project. More information on the UCAC project can be found at <http://ad.usno.navy.mil/ucac/>.

## REFERENCES

- Cutri, R.M. et al. 2003, Expl. Suppl. to the 2MASS All Sky Data Release, <http://www.ipac.caltech.edu/2mass/releases/allsky/doc/explsup.html>
- de Vegt, C., Hindsley, R., Zacharias, N., & Winter, L. 2001, AJ, 121, 2815
- de Vegt, C., Laux, U., & Zacharias, N. 2003, in *Small Telescopes in the New Millenium*, Vol.II, p.255, ed. T. Oswalt, Kluwer Acad.Publ.
- Douglass, G.G., & Harrington, R.S. 1990, AJ, 100, 1712

- Dunham, D. 2004 (in preparation for S&T)
- Evans, D.W. et al. 2003, Carlsberg Meridian Catalogue Number 13, Copenhagen, Cambridge, San Fernando
- Evans, D.W. et al. 2004 (in preparation)
- Høg et al. 2000, A&A, 355, L27
- IAU 2000, Hipparcos Celestial Reference Frame, in Proceedings of the Twenty-fourth General Assembly, Manchester, Resolution B1.2, 36
- Klemola, A.R., Jones, B.F., & Hanson, R.B. 1987, AJ, 94, 501
- Kroupa, P., & Bastian, U. 1997, New Astr. 2, 77
- Monet, D.G. et al. 2003, AJ, 125, 984
- Platais, I. et al. 1998, AJ, 116, 2556
- Rapaport, M., Le Campion, J.-F., Soubiran, C., Daigne, G., Périé, J.-P., Bosq, F., Colin, J., Desbats, J.-M., Ducourant, C., Mazurier, J.-M., Montignac, G., Ralite, N., Réquière, Y., & Viateau, B. 2001, A&A, 376, 325
- Schorr, R., Kohlschütter, A. 1951, *Zweiter Katalog der Astronomischen Gesellschaft*, AGK2, Volume I, Hamburg
- Stone, R., Pier, J.R., & Monet, D.G. 1999, AJ, 118, 2488
- Urban, S., Corbin, T.E., & Wycoff, G.L. 1998, AJ, 115, 2161
- Urban, S.E. et al. in preparation for AJ
- Winter, L. 1999, Ph.D. thesis, Hamburg Observatory
- Zacharias, N. & Zacharias, M.I. 1999, AJ, 118, 2503
- Zacharias, N., Urban, S. E., Zacharias, M. I., Hall, D. G., Wycoff, G. L., Rafferty, T. J., Germain, M. E., Holdenried, E. R., Pohlman, J. W., Gauss, F. S., Monet, D. G., & Winter, L. 2000, AJ, 120, 2131
- Zacharias, N. et al. 2003, in IAU 25th GA, Joint Discussion 16 proceedings, USNO, Washington DC, eds. R. Gaume, D. McCarthy, & J. Souchy
- Zacharias, N. 2002, in Proc. SPIE 4836, p.279, eds. T.A. Tyson & S. Wolff
- Zacharias, N. 2003, in *Small Telescopes in the New Millennium*, Vol.II, p. 67, ed. T. Oswalt, Kluwer Acad. Publ.
- Zacharias, N. et al. 2004, in preparation for AJ(extragalactic link of UCAC)

---

This 2-column preprint was prepared with the AAS L<sup>A</sup>T<sub>E</sub>X macros v5.2.

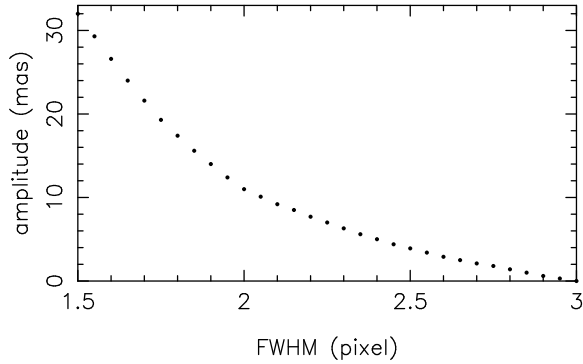


Fig. 1.— Amplitude as a function of image profile width (FWHM) for the position correction model as a function of pixel phase for CCD astrograph frames.

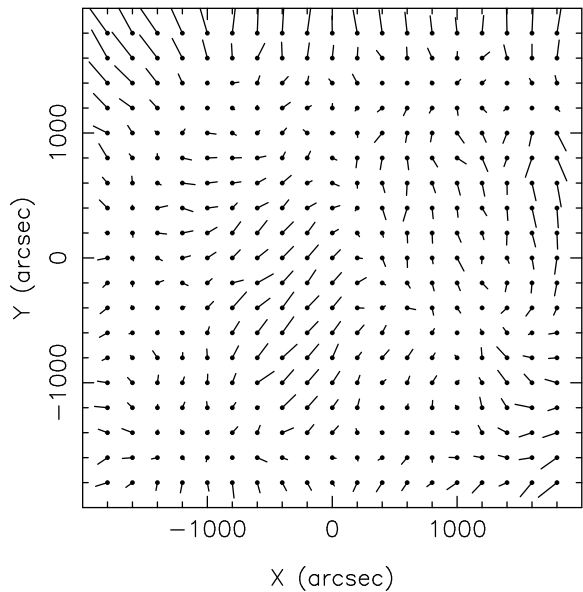


Fig. 2.— Field distortion pattern for CCD astrograph data taken at CTIO. The scale of the vectors is 10,000 which makes the largest correction vectors about 25 mas long.

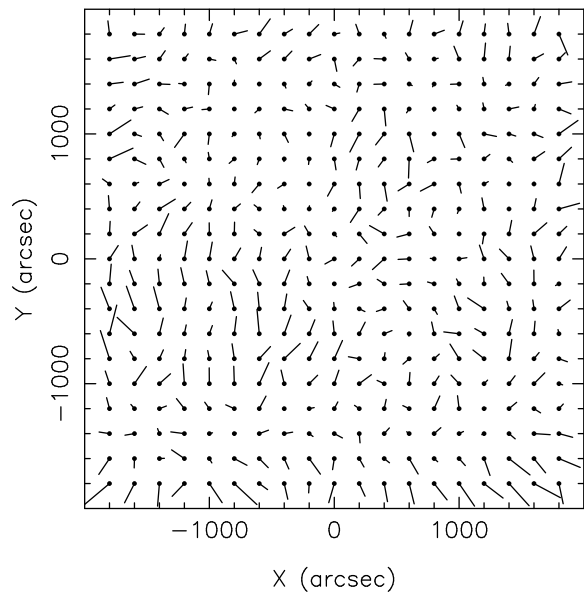


Fig. 3.— Field distortion pattern for CCD astrograph data taken at NOFS. The scale of the vectors is 10,000; which makes the largest correction vectors about 25 mas long. The much smaller number of available CCD frames cause the larger random scatter as compared to the previous figure.

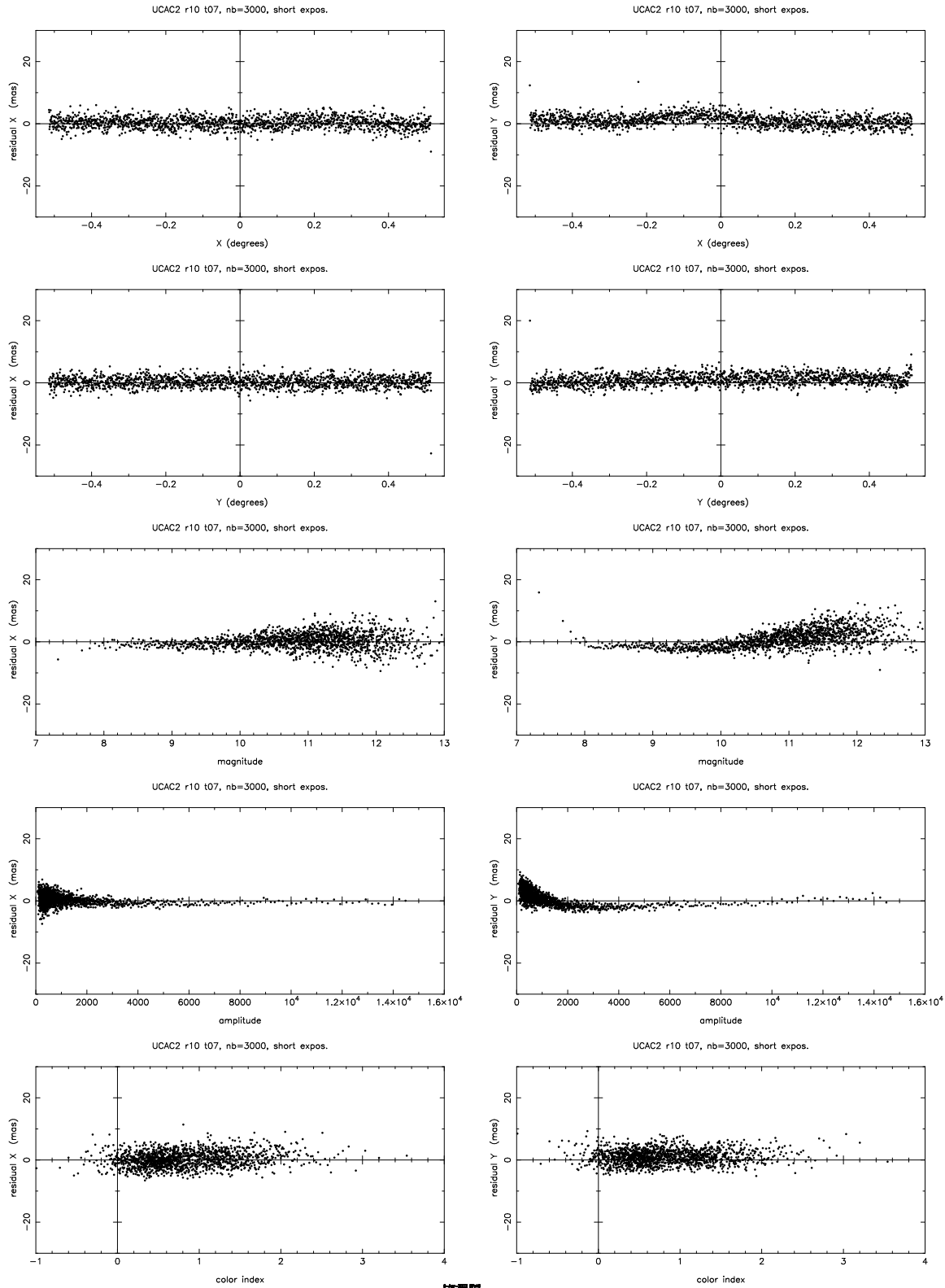


Fig. 4.— Residuals of CCD astrograph short exposures ( $\leq 40$  sec) taken at CTIO with respect to Tycho-2 reference stars. The left- and right-hand sides show  $x$  residuals (RA) and  $y$  residuals (Dec), respectively. From top to bottom residuals are shown as a function of  $x$ ,  $y$ , magnitude, amplitude, and color index. One dot represents the

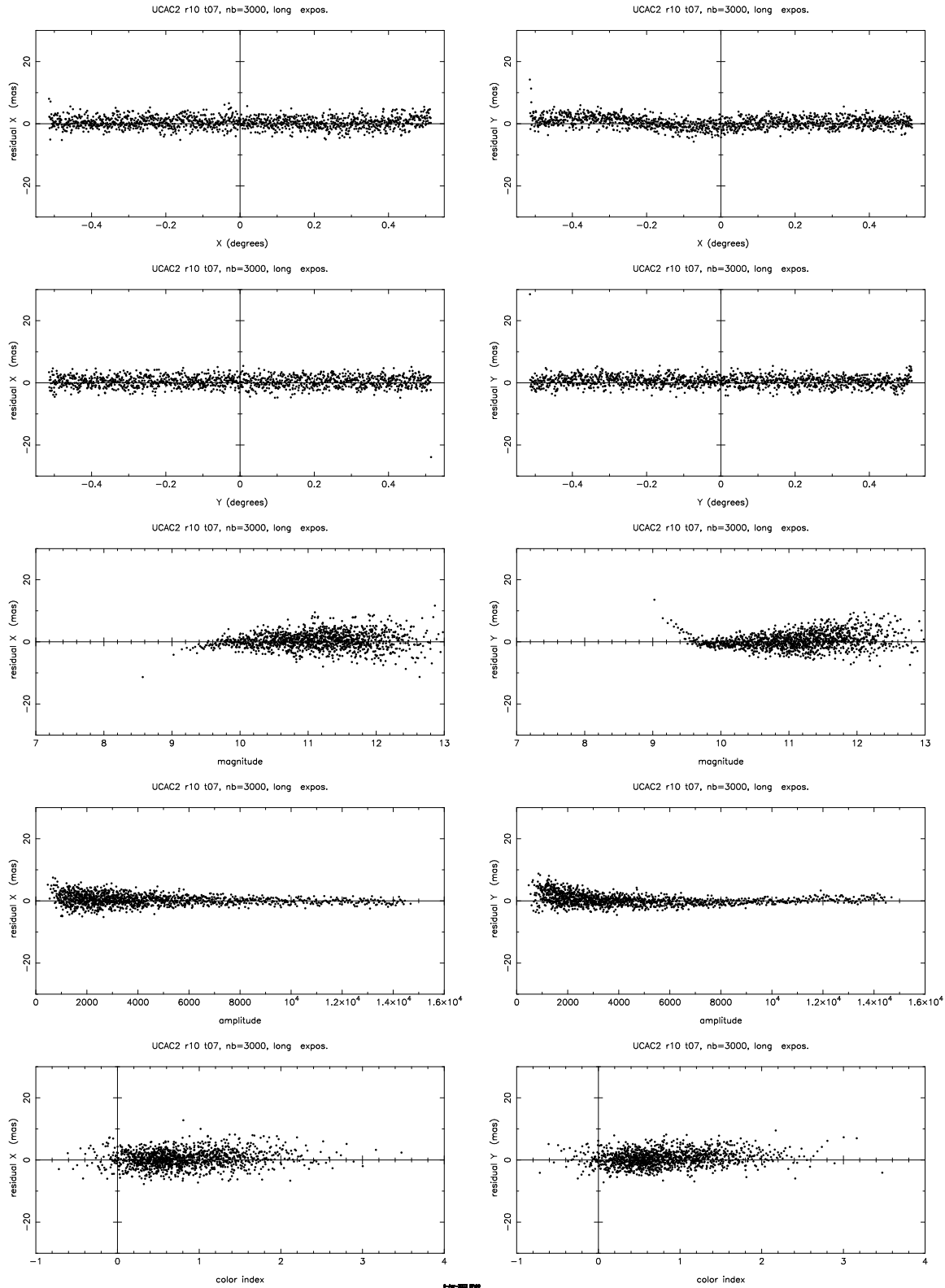


Fig. 5.— Residuals of CCD astrograph long exposures ( $\geq 100$  sec) taken at CTIO with respect to Tycho-2 reference stars, else as previous figure. Note, the long exposures saturate at about magnitude 9.5.

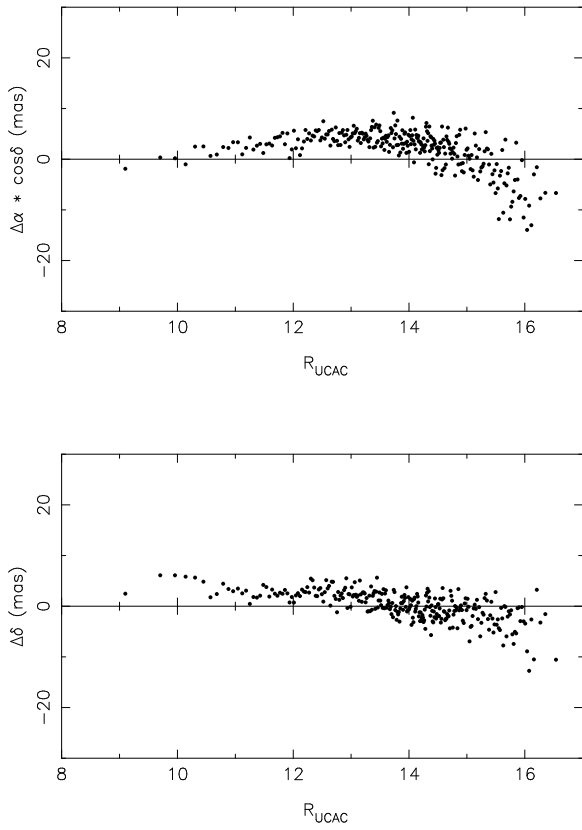


Fig. 6.— Position differences as a function of magnitude between observations with the CCD astrograph obtained from its CTIO and NOFS location of 130 fields in common. One dot represents the mean over 500 differences.

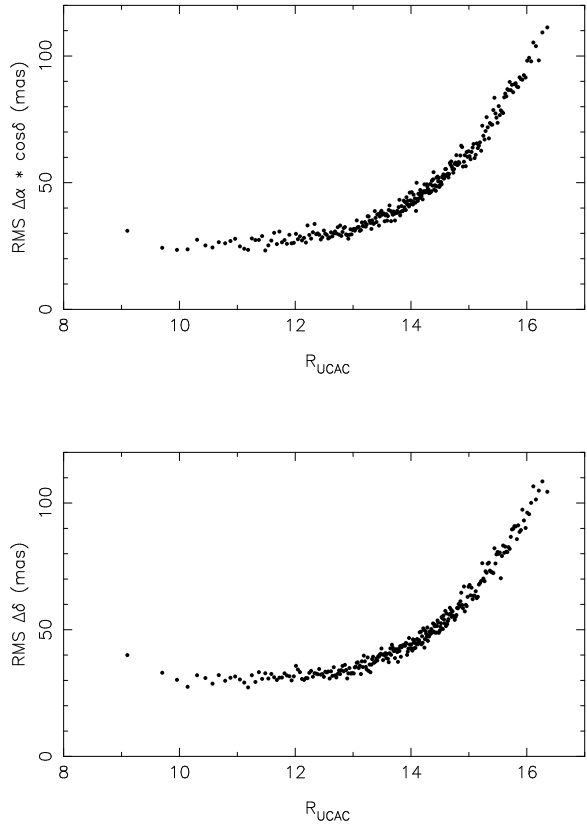


Fig. 7.— Same as previous figure, but RMS position differences are shown here.

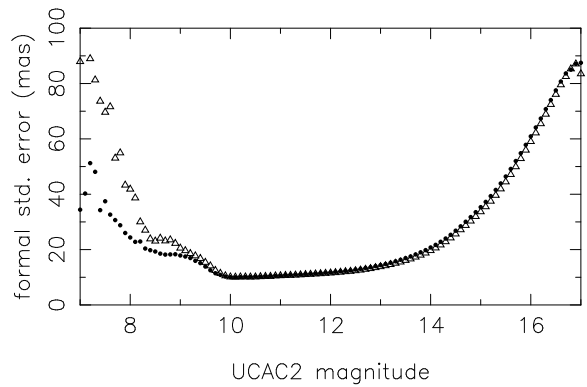


Fig. 8.— Precision of the CCD astrograph positions at their observational epoch. The filled dots and open triangles represent the RA and Dec component, respectively.

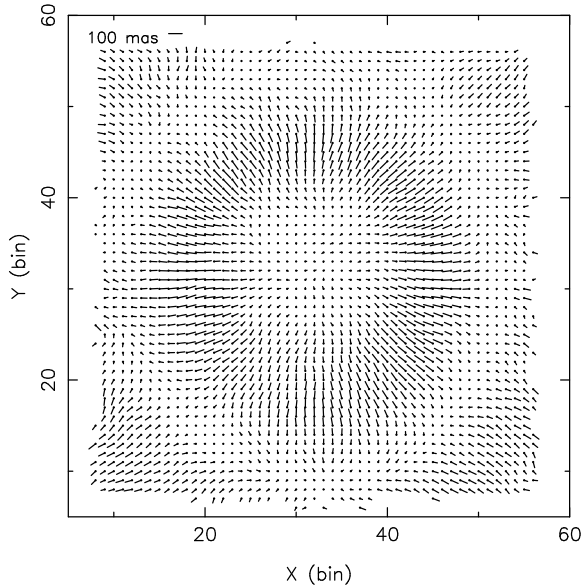


Fig. 9.— The field distortion pattern (FDP) of YS3 w.r.t. Tycho-2 astrometry prior to corrections. Shown is the NPM data covering all Tycho-2 magnitudes. The FDP changes with magnitude and survey. Largest vectors are  $\approx 100$  mas.

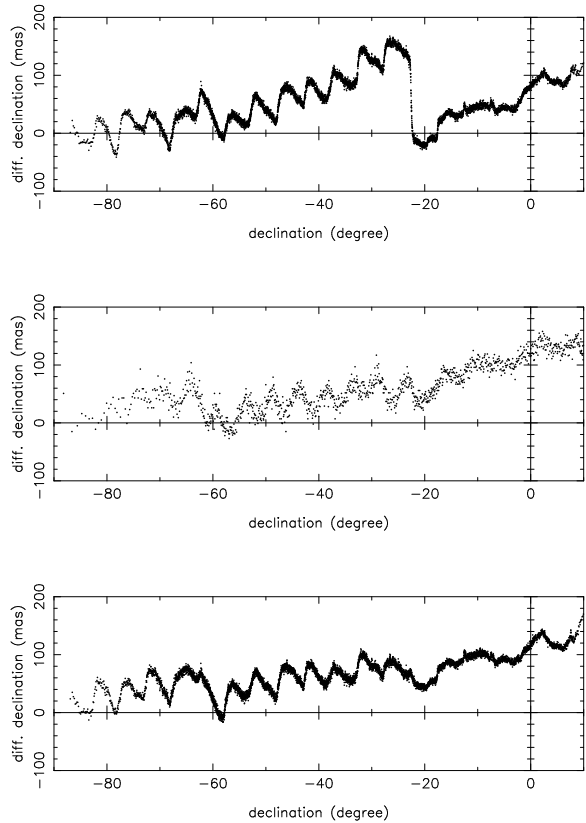


Fig. 10.— Differences in YS3 declination positions (post-FDP corrections) w.r.t. UCAC and Tycho-2 astrometry as a function of declination. No proper motions are applied, so the data are not expected to be near zero, but instead show galactic and solar motion. Each data point is a mean of 4,000 differences for the top and bottom and 1,000 for the middle diagram. The top diagram shows the initial YS3–UCAC2 differences with a discontinuity near  $-25^\circ$ , which is at the boundary of the NPM and SPM data. The middle figure contains similar data but using Tycho-2. A much smaller discontinuity is seen, which is likely a result of the different epochs between the NPM and SPM observational data. The figure at the bottom shows the same data as the top, but following zero-point corrections of the SPM and NPM plates. The higher frequency oscillations in the southern data of 30 to 50 mas appear to be systematic errors on the individual plate level. They have been investigated but remained unexplained.

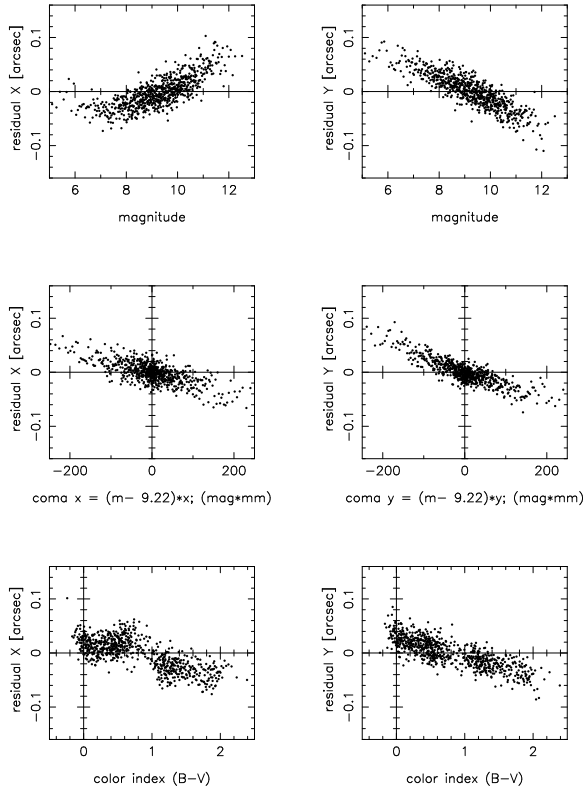


Fig. 11.— Systematic errors in the subset of Hamburg Zone AGK2 plates. Binned (200) residuals with respect to Hipparcos reference stars from a preliminary reduction are shown. The left-hand side shows residuals in  $x$  (RA), the right-hand side those for  $y$  (Dec). From top to bottom residuals are displayed as a function of magnitude, coma-term, and color index, respectively.

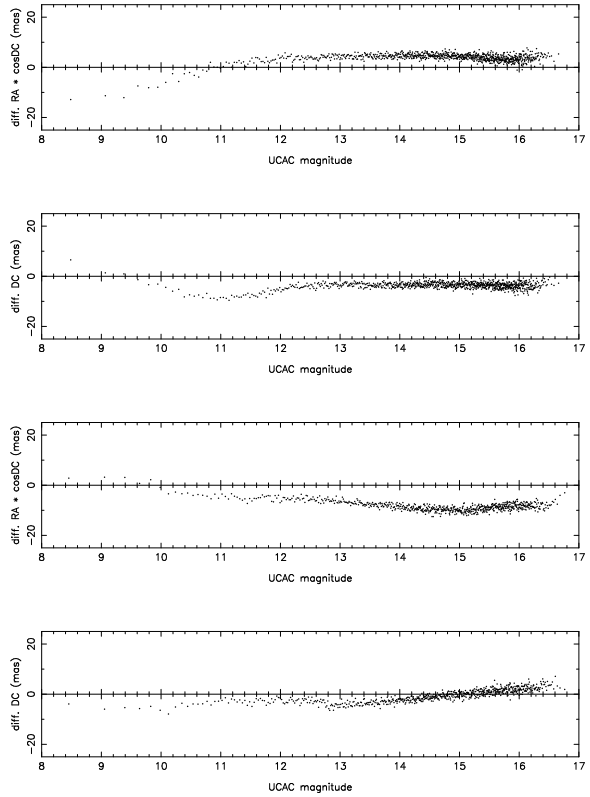


Fig. 12.— UCAC2 minus 2MASS position differences as a function of UCAC magnitude for the declination zone  $-40^\circ$  to  $-30^\circ$  (top 2 diagrams) and  $+30^\circ$  to  $+40^\circ$  (bottom). One dot represents the mean over 5,000 stars.

UCAC: 10275 survey fields completed as of December 8, 2002

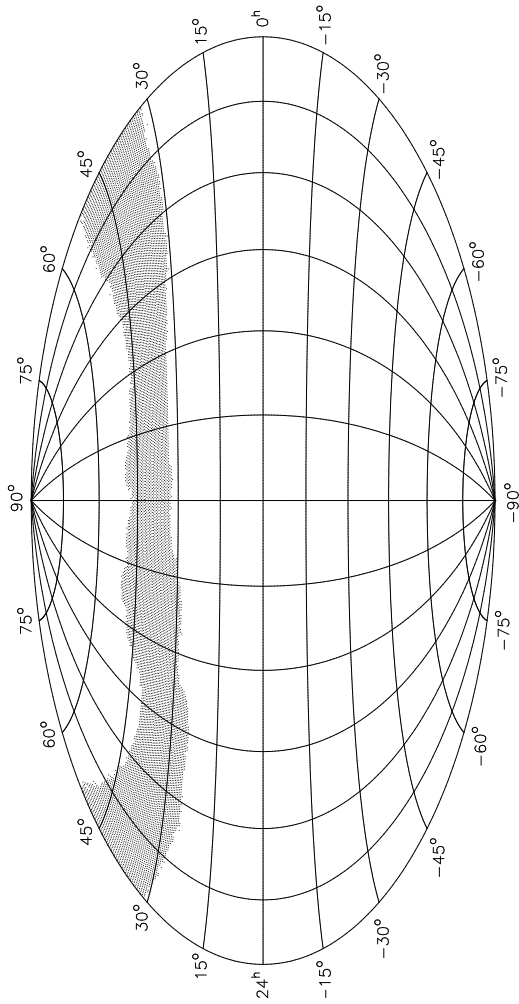


Fig. 13.— Sky coverage of UCAC2 observations from the NOFS location. All sky south of the band shown was completed from the CTIO location. UCAC2 covers a total of 86% of the sky.

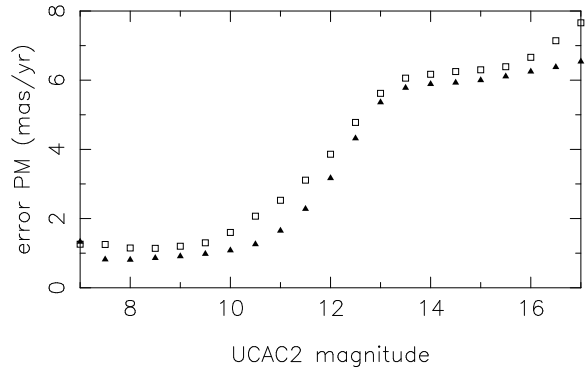


Fig. 14.— Mean, formal errors of UCAC2 proper motions (per coordinate) as a function of magnitude. The open squares and filled triangles are for the southern and northern hemisphere, respectively.

Table 1: Overview of the telescope, camera, and astrograph observing.

Parameter	value
Clear aperture	206 mm
Focal length	2057 mm
Field of view	$\approx 9^\circ$
Number of pixels	4094 x 4094
Pixel size	9.0 $\mu\text{m}$
Sampling	0.9 "/pixel
Field of view	61' x 61'
Spectral bandpass	579–642 nm
Readout	14 bit, 16 sec
Frames per field	1 long + 1 short
Exposure times	25 + 125 sec
Overlap pattern	2-fold (fields)
All sky	85,158 fields
Limiting magnitude	$\approx 16$
Fields per hour	$\approx 12$
Typical night	3.0 GB compressed

Table 2: Milestones of the UCAC project.

Date	Activity
1997 Jan	4k camera arrives at Washington
1998 Jan 10	first light at CTIO
1998 Feb 13	begin of survey observing
1999 Feb 13	24 % of sky complete
2000 Feb 13	44 % of sky complete
2000 Mar	release of UCAC1
2000 Apr 30	50 % of sky complete
2000 Aug 26	southern hemisphere complete
2001 Sep 18	last night at CTIO
2001 Oct 31	begin survey observing at NOFS
2002 Mar 01	200,000 frames taken
2002 Dec 07	cut for UCAC2 data = 86 % of sky
2003 July	release of UCAC2 at IAU GA
2004 May	expected full sky coverage
2005	expected UCAC3 release

Table 3: Parameters for position corrections due to low CTE as a function of exposure time  $t$  (sec). The  $c$  and  $d$  parameters are for the  $x$  and  $y$  coordinate, respectively (see text). The  $-6$  and  $-9$  stand for  $10^{-6}$  and  $10^{-9}$ , respectively for units of magnitude and pixel.

$t$	$c_1$	$c_2$	$c_3$	$c_4$	$d_1$	$d_2$	$d_3$	$d_4$
	-6	-6	-9	-9	-6	-6	-9	-9
5	6.5	0.80	-10	0.20	3.3	0.10	20	-0.50
10	6.5	0.80	-10	0.20	3.3	0.10	20	-0.50
20	6.1	0.79	-10	0.25	3.2	0.10	20	-0.50
25	6.3	0.81	-25	0.25	3.1	0.10	15	-0.50
30	6.3	0.83	-50	0.25	2.8	0.10	15	-0.50
40	6.2	0.65	-60	0.30	2.5	0.05	15	-0.40
60	6.0	0.60	-70	0.30	1.8	0.00	20	-0.35
80	5.8	0.55	-80	0.30	1.6	0.00	30	-0.30
100	5.3	0.52	-95	0.40	1.4	-0.10	35	-0.25
125	5.0	0.44	-100	0.45	1.3	-0.10	35	-0.23
150	4.7	0.40	-100	0.55	1.2	-0.12	35	-0.22
200	4.6	0.33	-95	0.45	0.9	-0.09	25	-0.15

Table 4: Modifying factors  $k_s$  and  $k_l$  for long and short exposures, respectively, to be applied to the  $c$  and  $d$  parameters of the previous table for position corrections due to the low CTE.

FWHM (arcsec)	$k_s$	$k_l$
1.5	0.96	1.00
1.6	1.00	1.00
1.7	1.04	1.00
1.8	1.08	1.04
1.9	1.11	1.09
2.0	1.14	1.14
2.2	1.23	1.18
2.4	1.36	1.21
2.6	1.50	1.23
2.8	1.60	1.25
3.0	1.70	1.27

Table 5: Corrections for  $x, y$  positions for bright stars (near saturation) as a function of fit image profile amplitude.

amplitude (counts)	$\Delta x$ (mas)	$\Delta y$ (mas)
13000	0	4
14000	0	10
15000	-1	27
16000	-3	62
17000	-6	130
18000	-9	77
19000	-12	89
20000	-15	87
22000	-18	60
24000	-21	30

Table 6: Slope of color dependent residuals of AGK2 plate data.

Zone	$x$ (mas/mag)	$y$ (mas/mag)	mean (B-V)
Bonn	-160	-226	0.85
Hamburg	-35	-36	0.80

Table 7: Systematic offsets of UCAC2 proper motions as derived from external comparisons.

$\Delta\mu_\alpha \cos \delta$ (mas/yr)	$\Delta\mu_\delta$ (mas/yr)	numb. sources	data set
+0.2	-1.0	200	LMC stars (2MASS color selected)
+1.3	-0.8	1300	SPM2 galaxies ( $-47^\circ.. -21^\circ$ decl.)
-0.7	-0.0	52000	stars from ERLcat ( $11.5$ to $14.5^m$ )
+0.3	-0.6		average over all 3 sets

Table 8: Systematic differences between UCAC2 and ERLcat proper motions as a function of declination zone. The  $\sigma$  columns give the scatter in the observed proper motion differences, while f.e. are the corresponding formal errors. The last 2 columns give the mean of the normalized ( $\Delta\mu/\sigma_\mu$ ) proper motion differences.

numb. stars	declin. zone	mean mag	$\Delta\mu_\alpha \cos \delta$ (mas)	$\Delta\mu_\delta$ (mas)	$\sigma_{\Delta\mu_\alpha \cos \delta}$ (mas)	$\sigma_{\Delta\mu_\delta}$ (mas)	f.e. $\Delta\mu_\alpha \cos \delta$ (mas)	f.e. $\Delta\mu_\delta$ (mas)	normal. $\Delta\mu_\alpha \cos \delta$	normal. $\Delta\mu_\delta$
3588	-90 - 60	12.7	-1.7	-0.4	12.3	8.4	7.7	7.6	-0.26	-0.07
10743	-60 - 30	12.8	-0.9	+1.0	8.5	7.5	6.7	6.7	-0.15	+0.15
22918	-30 + 10	13.0	-0.8	-0.3	8.9	8.7	7.9	7.8	-0.08	-0.04
18927	+10 + 55	12.8	-0.5	-0.4	7.8	7.2	6.4	6.4	-0.10	-0.09
52588	-60 + 60	12.9	-0.7	-0.0	8.4	7.9	7.2	7.1	-0.10	-0.01

Table 9: Contents and format of a UCAC2 binary data record. Numbers in parentheses refer to 15 notes and are explained in the “readme” file, which is found on each CD and the project Web page.

Num	Bytes	Fmt	Unit	Label	Explanation
1	1- 4	I*4	mas	RA	Right Ascension at epoch J2000.0 (ICRS) (2)
2	5- 8	I*4	mas	DE	Declination at epoch J2000.0 (ICRS) (2)
3	9-10	I*2	0.01 mag	U2Rmag	Internal UCAC magnitude (red bandpass) (3)
4	11	I*1	mas	e_RA	s.e. at central epoch in RA (*cos DEm)(1,4)
5	12	I*1	mas	e_DE	s.e. at central epoch in Dec (1,4)
6	13	I*1		nobs	Number of UCAC observations of this star(5)
7	14	I*1		e_pos	Error of original UCAC observ. (mas) (1,6)
8	15	I*1		ncat	# of catalog positions used for pmRA, pmDC
9	16	I*1		cflg	ID of major catalogs used in pmRA, pmDE (7)
10	17-18	I*2	0.001 yr	EpRA	Central epoch for mean RA, minus 1975 (8)
11	19-20	I*2	0.001 yr	EpDE	Central epoch for mean DE, minus 1975 (8)
12	21-24	I*4	0.1 mas/yr	pmRA	Proper motion in RA (no cos DE) (9)
13	25-28	I*4	0.1 mas/yr	pmDE	Proper motion in DE (9)
14	29	I*1	0.1 mas/yr	e_pmRA	s.e. of pmRA (*cos DEm) (1)
15	30	I*1	0.1 mas/yr	e_pmDE	s.e. of pmDE (1)
16	31	I*1	0.05	q_pmRA	Goodness of fit for pmRA (1,11)
17	32	I*1	0.05	q_pmDE	Goodness of fit for pmDE (1,11)
18	33-36	I*4		2m_id	2MASS pts_key star identifier (12)
19	37-38	I*2	0.001 mag	2m_J	2MASS J magnitude (13)
20	39-40	I*2	0.001 mag	2m_H	2MASS H magnitude (13)
21	41-42	I*2	0.001 mag	2m_Ks	2MASS K_s magnitude (13)
22	43	I*1		2m_ph	2MASS modified ph_qual flag (1,14)
23	44	I*1		2m_cc	2MASS modified cc_flg (1,15)

Table 10: Example UCAC2 data for the first 5 stars. The columns are split over 2 blocks for easier reading.

item	1	2	3	4	5	6	7	8	9	10	11	12
1246420	-322767602	1591	75	87	2	97	2	1	17330	15213	31020	
4125230	-323707012	1382	15	28	8	21	2	1	23246	22659	134316	
7345118	-322447512	1579	24	26	4	25	2	1	22903	22799	45845	
8139385	-322284308	1479	53	25	5	41	2	1	20455	22911	18125	
11128880	-323115466	1631	15	43	2	27	2	1	23364	21562	39404	
item	13	14	15	16	17	18	19	20	21	22	23	
	-35	70	74	20	20	1229086517	14428	13865	13751	000	000	
	-187	61	62	20	20	1101364107	12467	12131	11963	000	000	
	104	61	62	20	20	1329022468	14169	13752	13708	220	000	
	-16	65	61	20	20	1085341332	13111	12511	12339	000	000	